Int. J. Electrochem. Sci., 7 **(2012)** 6154 - 6167

International Journal of ELECTROCHEMICAL SCIENCE
www.electrochemsci.org

Coating Electrospun Polyvinyl Alcohol and Polyvinyl Chloride Fibers As Corrosion Passivation Applications

El-Sayed M. Sherif 1,4, Mahir Es-saheb[2,], Ahmed El-Zatahry [3,5], El-Refaie kenawyand and Ahmad S. Alkaraki[2]*

[1] Center of Excellence for Research in Engineering Materials (CEREM), Advanced Manufacturing Institute, King Saud University, P. O. Box 800, Riyadh 11421, Saudi Arabia
[2] Mechanical Engineering Department, King Saud University, P.D. Box 800, Riyadh 11421, Saudi Arabia
[3] Petrochemical Research Chair, Chemistry Department, College of Science, King Saud University, B.O. Box 2455 Riyadh 11451, Saudi Arabia
[4] Electrochemistry and Corrosion Laboratory, Department of Physical Chemistry, National Research Centre (NRC), Dokki, 12622 Cairo, Egypt
[5]Advanced Technology and New Materials Research Institute, City of Scientific Research and Technology Applications, New Boarg El-Arab City, Alexandria, Egypt.
[6] Chemistry Department, Polymer Research Group, Faculty of Science, Tanta University, Tanta 31527, Egypt.
[*]E-mail: essaheb@ksu.edu.sa

Received: 23 May 2012 / *Accepted:* 7 June 2012 / *Published:* 1 July 2012

Two nanofiber coatings, namely polyvinyl alcohol (PVA) and polyvinyl chloride (PVC) were prepared and deposited on aluminum surface using electrospinning technology. The coating layers were characterized using thermogravimetric analysis (TGA), optical (OM) and scanning electron (SEM) microscopes. The SEM images showed that the deposited PVA and PVC coatings on the aluminum surface have a compact and entangled nanofiber structure with diameters varied from 100 to 199 nm in case of PVA/Al, and from 150 to 400 nm in case of PVC/Al. The electrochemical corrosion of aluminum without and with PVA and PVC coatings in freely aerated stagnant solutions of 3.5 wt.% sodium chloride (NaCl) was investigated using cyclic potentiodynamic polarization (CPP) and electrochemical impedance spectroscopy (EIS) measurements. It has been found that the deposited PVA and PVC coatings decrease the corrosion currents and corrosion rate as well as increase the corrosion resistance for aluminum in the NaCl solution. Results together were in good agreement and confirmed that the deposited PVA and PVC coatings highly protect the aluminum versus corrosion in the chloride test solutions.

Keywords: aluminum corrosion; corrosion protection, electrospinning; impedance spectroscopy; polarization; polymeric coatings

1. INTRODUCTION

Electrospinning is a unique technology that has been widely used in many applications in varied industrial fields. The method is successfully used in medical, engineering, energy, nano-industry, and others applications [1-3]. The deposition of polymers by electrospinning test produces nano-woven fibrous structures with fiber diameters ranging from tens of nanometers to microns. At these conditions, the materials earn excellent properties like large surface area to volume ratio, flexibility in surface functionalities, and superior mechanical performance [3-6].

A nanocomposite coating is a composite material with at least two phases: a nanocrystalline phase and a matrix (amorphous/non-amorphous) phase, or two nanocrystalline phases. The ability to reinforce fine particulate matter such as hard ceramic particles within metal or polymer matrix has led to the development of nanocomposite coatings. These coatings exhibit superior properties compared to the plain non-composite ones. The driving force for the advancement in nanocomposite coatings has been an improvement in corrosion and wear resistance. The aim has been to enhance reliability and performance of various structural components to enable them to resist corrosion, pitting, exfoliation, erosion, sliding and wear. Corrosion and wear resistant coatings can be used in a variety of industries such as in automobile, power generation, utility, aerospace, defense, optical equipment, magnetic storage devices and bearings, engine parts and seals, etc [7-13].

Recently, there are several processing techniques have been used to prepare polymer nanofibers; some of these are: drawing, template synthesis, phases separation, self-assembly, and electrospinning [14-18]. Due to a large number of possible combinations between particulate material and the matrix, a wide variety of technological applications can be met by nanocomposite coatings [19]. Appropriate nanocomposite coatings can also act as a barrier to protect underlying substrate material from corrosion. Nickel is one of the most widely used elements for coatings due to its wide ranging applications such as heat sinks, gears, carburetor components (automotive), compressor blades, piston heads, gyro parts (aircraft), pressure vessels, pumps, heat exchangers (chemical), connectors, interlocks,(electrical), moulds, grills (food) as well as dozens of other applications in numerous industries [20]. Hard ceramic composite coatings have also attracted considerable attention due to their unique properties. Nanocomposite coatings exhibit hardness significantly exceeding that given by the rule of mixture, along with high toughness. Nanocoatings can have a hardness ranging from 20 GPa (classified as Hard) to 40 GPa (Super-hard) up till 80 GPa (Ultra-hard) [21].

The objective of our current investigation was to synthesize then apply a nanofiber coating of polyvinyl alcohol (PVA) and polyvinyl chloride (PVC) on the pure aluminum surface using the electrospinning deposition technique. The objective was also extended to report the effect of PVA and PVC on the corrosion resistance of aluminum in freely aerated solutions of 3.5 wt. % NaCl. A variety of electrochemical and surface analysis techniques have been employed in this work. These included the use of cyclic potentiodynamic polarization and electrochemical impedance spectroscopy measurements along with a scanning electron microscope and thermogravimetric analysis.

2. MATERIALS AND EXPERIMENTAL TECHNIQUES

2.1. Electrospinning deposition of polymer coatings

Two different polymer solutions were prepared for electrospinning process. The first solution, 10 wt. % PVA, was prepared by mixing 10 g PVA pellets at 50 $^{\circ}$C with distilled water to make 100 ml, then stirring the mix overnight. The second polymer solution, 10 wt. % PVC, was prepared by dissolving the polymer pellets in a tetrahydrofuran (THF) solvent at room temperature under stirring overnight. Prepared solutions electrospun at 15-kV positive voltage, 15-cm working distance, and 0.3-mL/h solution flow rate. The electrospun nanofibers were collected on aluminum foil surfaces, air dried in a hood at room temperature for overnight, then quickly rinsed in distilled water, and finally dried under vacuum oven at room temperature overnight.

2.2. Nanofibers morphological characterization

Surface morphology, diameter size and thickness of electrospun nanofibers coating layers on aluminum surfaces were investigated using scanning electron microscopy (JSM-7100F). After sputter coating with Gold, the fiber size distribution was measured up to five frames of randomly selected SEM micrograph using software.

2.3. Thermogravimetric Analysis

Thermo gravimetric analysis was carried out using a TA Instruments, Q500 TGA, using platinum cell in nitrogen atmosphere 20 ml/min.

2.4. Corrosion techniques

A 3.5 wt.% NaCl solution was prepared by dissolving 35 g of NaCl in 1 L glass flask. The PVA and PVC aluminum coated and non coated samples for corrosion measurements were prepared by attaching an insulated copper wire to one face of the sample using an aluminum conducting tape, and then isolated by cold mounted in resin before letting it to dry in air for 24 h at room temperature. The area of the other face of the samples, on which the measurements were carried out, was 1.0 cm^2.

Electrochemical experiments were performed by using a PARC Parstat-2273 Advanced Electrochemical System after immersing the bare and coated PVC electrodes for 20 minutes in freely aerated stagnant 3.5 wt.% NaCl solutions. The cyclic potentiodynamic polarization (CPP) curves were obtained by sweeping the potential from -1800 mV in the positive direction up to -500 mV vs. Ag/AgCl at a scan rate of 1 mV/s. The potential was scanned in the reverse direction from -500 mV (Ag/AgCl) at the same scan rate. For electrochemical impedance spectroscopy (EIS) experiments, the frequency was scanned at the open-circuit potential from 100 kHz to 0.1 Hz with an ac wave of ±5 mV peak-to-peak overlaid on a dc bias potential, and the Nyquist plots were acquired using Powersine software at a rate of 10 points per decade change in frequency.

3. RESULTS AND DISCUSSION

3.1. Surface morphology investigations

The surface morphology for (a) uncoated aluminum, (b) PVA coated aluminum and (c) PVC coated aluminum are shown respectively in Fig. 1. All these images were taken using high resolution digital camera. It is clearly seen from Fig. 1 that the PVA and PVC layers are compact and look homogeneously distributed on the surface.

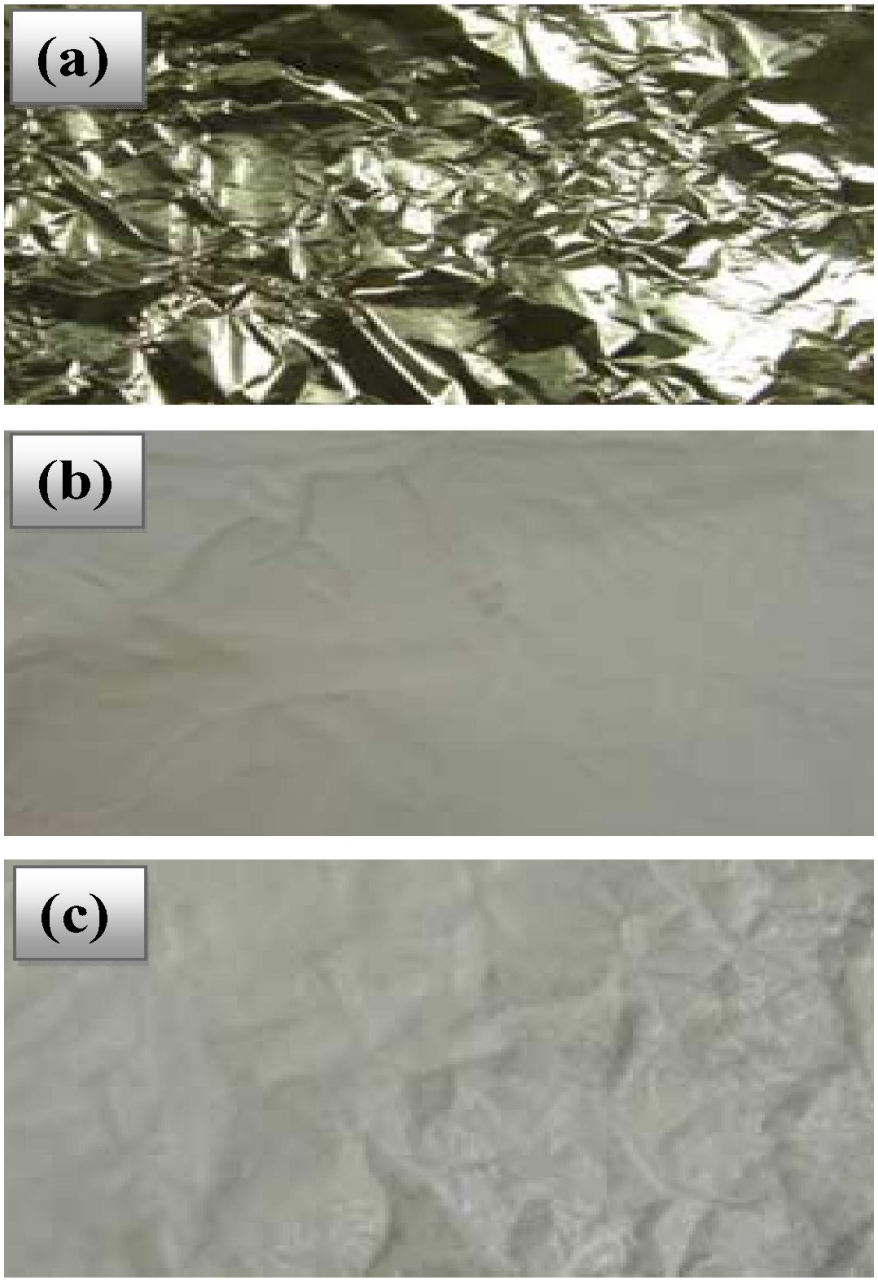

Figure 1. The digital images for (a) uncoated aluminum, (b) PVA coated aluminum and (c) PVC coated aluminum.

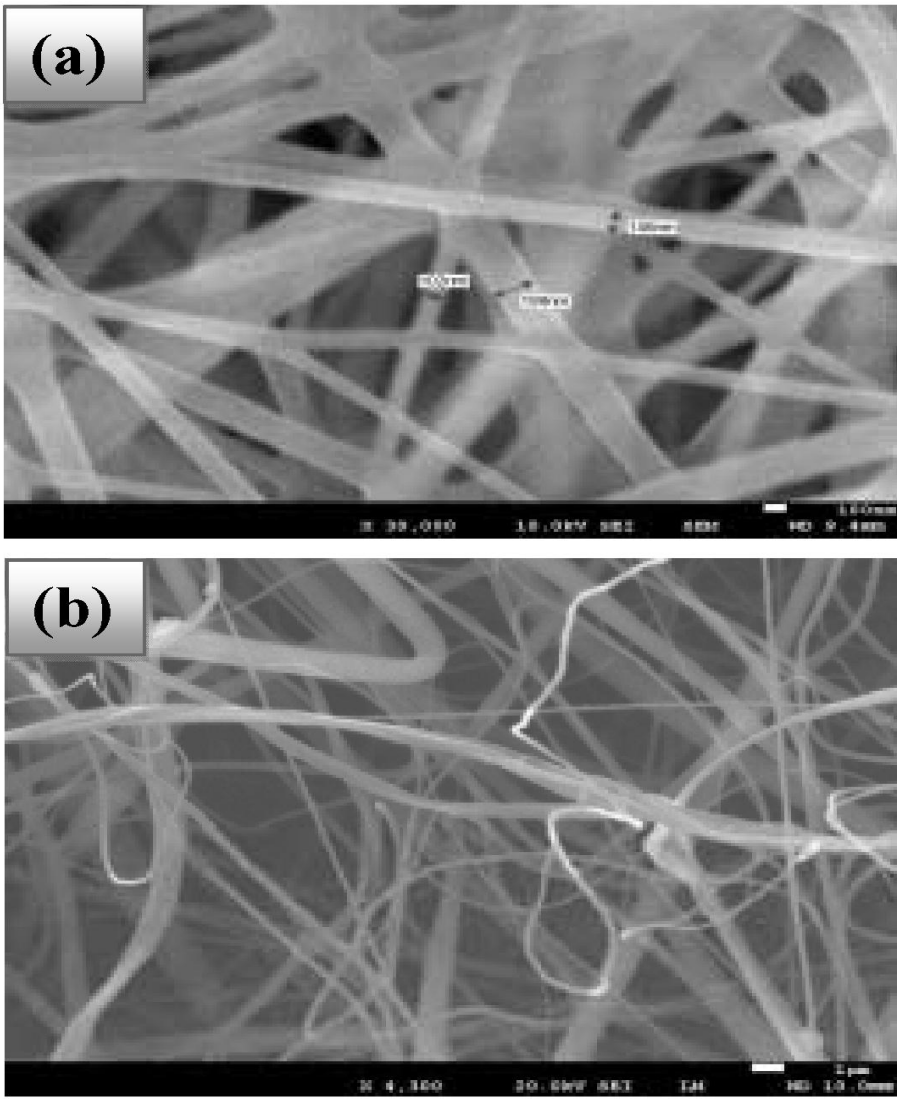

Figure 2. SEM images for (a) PVA and (b) PVC electrospun fiber coated over Aluminum substrates.

The morphology of the coated (a) PVA and (b) PVC films on aluminum was also examined using scanning electron microscopy (SEM) and the images are shown respectively in Fig. 2. A typical SEM image, Fig.2a, exhibits a web of randomly oriented fiber with a broad distribution from 100 to 199 nm in case of the PVA / Al sample. The SEM image, Fig. 2b, also shows a web of randomly oriented fiber with a broad distribution from 150 to 400 nm in the case of PVC/Al sample.

In order to report the thickness of the coated PVA and PVC layers on aluminum surface, the SEM side view images were taken as depicted by Fig. 3a and Fig. 3b, respectively. It is clearly seen from Fig. 3a that the coated film using PVA electrospun fiber is a homogenous, compact and dense layer with the average thickness size of about 190 μm. On the other hand, Fig. 3b displays that the formed layer using a PVC coating are non homogenous and has an average thickness size nearly 180 μm.

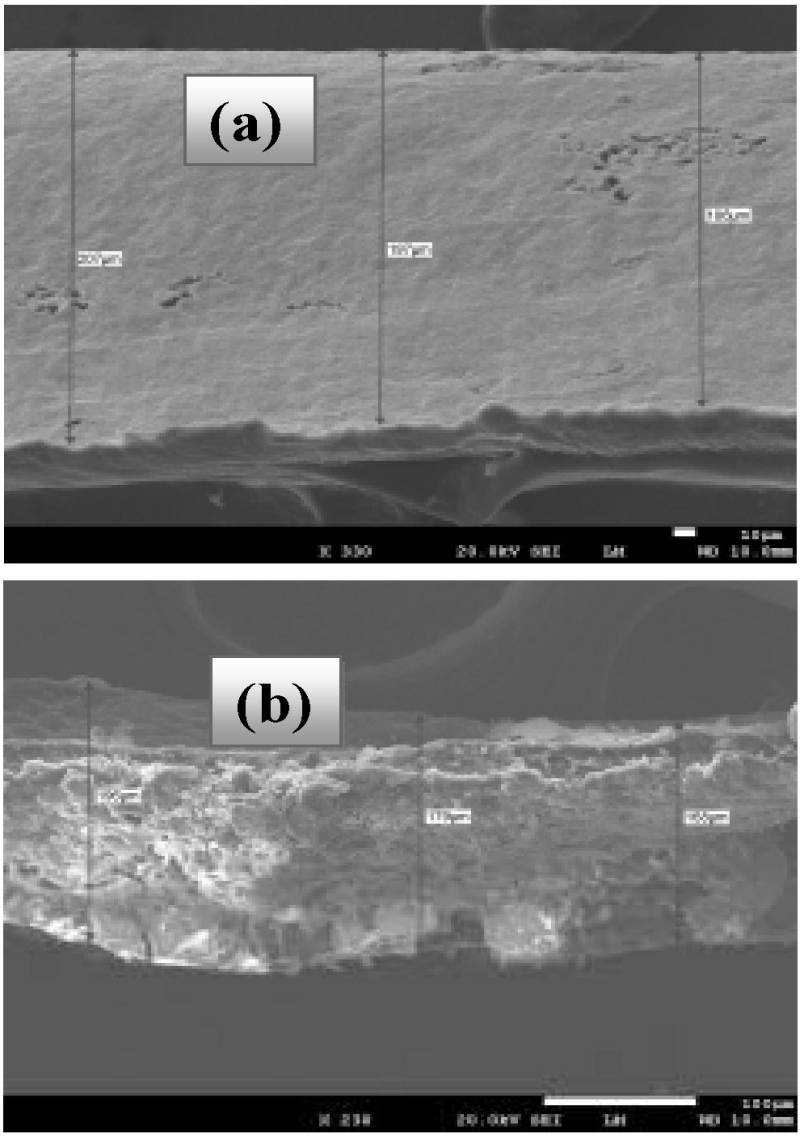

Figure 3. SEM micrographs of (a) PVA and (b) PVC electrospun fiber film over aluminum substrate (Side View)**.**

3.2. Thermogravimetric analysis

A comparison of prepared nanofibers thermal behavior is depicted in Fig. 4, which shows The TGA thermogram in a nitrogen atmosphere for electrospun PVA and PVC fibers. Results indicated that both of PVA and PVC electrospun fibers decompose in three stages. For PVA, the first stage at 30.09 – 200.00 $^{\circ}$C is related to the weight loss, while in the case of PVC at 29.51 - 170 $^{\circ}$C is due to the loss of humidity water and the water of crystallinity. The second stage at 200 -347 $^{\circ}$C in the case of PVA results from the weight loss, on the other hand the second stage for PVC appears at 220 - 336.80 $^{\circ}$C because of the dechloronation and the formation of intermediate. At last, the third stage for PVA takes place at 350-485 $^{\circ}$C due also to the weight loss. That stage appears for PVC 400.00 - 450.50 $^{\circ}$C

and might have resulted due to the decomposition to carbon oxide and volatile hydrocarbons. The complete TGA thermogram for PVC has also been reported in our previous work [1].

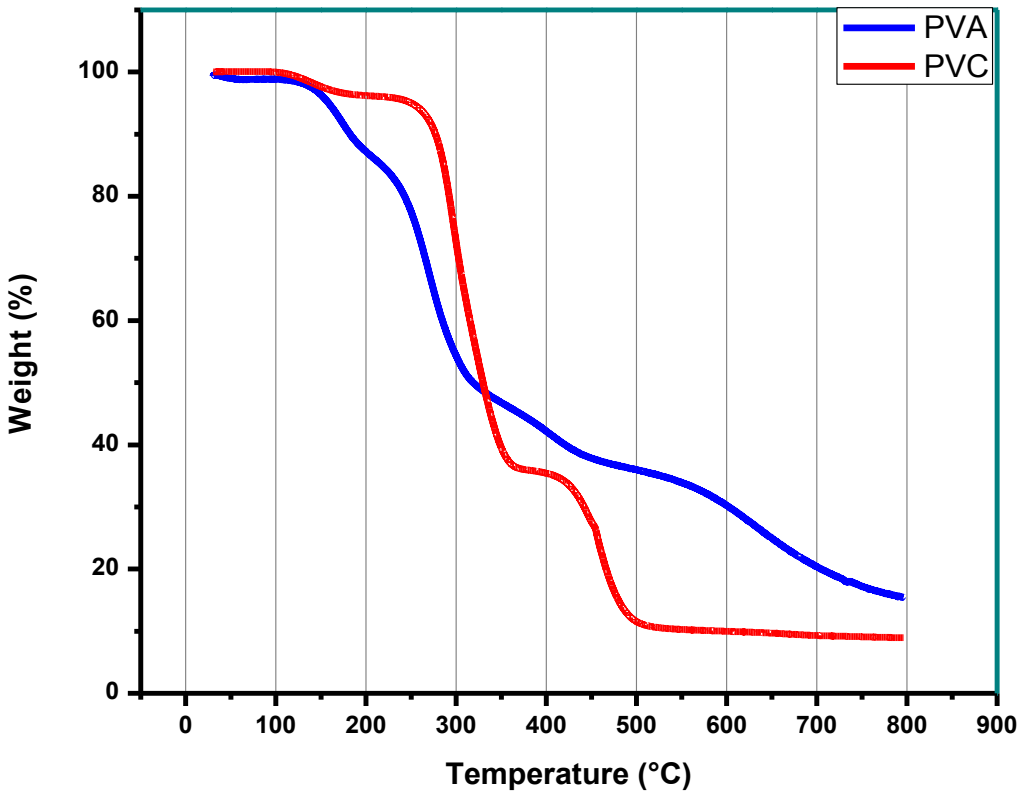

Figure 4. The TGA-thermogram in nitrogen atmosphere for electrospun PVA and PVC fibers.

3.3. Electrochemical impedance spectroscopy (EIS) measurements

The EIS is a powerful technique that has been employed to explain the corrosion and corrosion protection of metals and alloys including aluminum and its alloys in corrosive media such as chloride solutions [22-36]. Our EIS measurements were carried out to determine kinetic parameters for electron transfer reactions at the interface of the aluminum (without and with coatings) and the chloride solution. Typical Nyquist impedance plots obtained for (a) Al, (b) PVA coated Al, and (c) PVC coated Al electrodes at an open-circuit potential after 20 min immersion in 3.5 wt.% NaCl solutions are shown in Fig. 5. The Nyquist plots shown in Fig. 5 were fitted to the best equivalent circuit model as shown in Fig. 6; this circuit has also been used in similar conditions for aluminum in chloride solutions as reported in our previous studies [24,28]. The values of the parameters obtained by fitting the equivalent circuit shown in Fig. 6 are listed in Table 1. According to usual convention, R_S represents the solution resistance between aluminum electrodes and the counter (platinum) electrode, Q_1 and Q_2 the constant phase elements (CPEs), R_{P1} the resistance of a film layer formed on the surface of aluminum, R_{P2} accounts for the polarization resistance at the aluminum surface, and W the Warburg impedance.

It is clearly seen from Fig. 5 that the aluminum electrode shows a distorted single semicircle regardless of whether the surface is coated or not. The aluminum coated PVA surface showed a bigger diameter for the semicircle; this effect increases in the case of PVC coated aluminum surface. This is due to the increased surface passivation by PVA and further protection was obtained for PVC coated aluminum. It has been reported that [37-41] the semicircles at high frequencies are generally associated with the relaxation of electrical double layer capacitors and the diameters of the high frequency semicircles can be considered as the charge transfer resistance. On the other hand, the diameter of the semicircle for Al at low frequency also increased for the coated PVA and PVC surfaces [22-26]. The presence of PVA and PVC on the aluminum surface thus increases the impedance of aluminum through increasing its surface passivation. This effect for PVA and PVC decreases the electrochemical active and flawed areas on the aluminum surface due to their being compact and highly adherent to the aluminum surface.

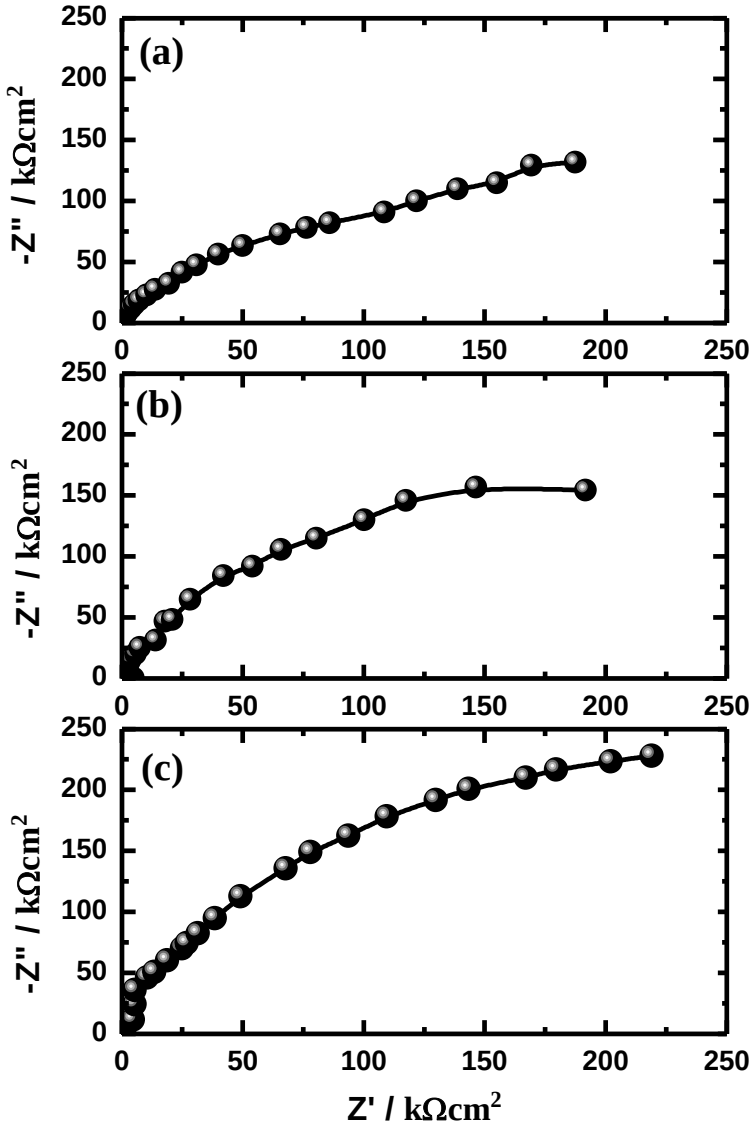

Figure 5: EIS Nyquist plots obtained for (a) Al, (b) Al coated with PVA, and (c) Al coated with PVC electrodes after their immersion for 20 min in freely aerated 3.5 wt.% NaCl solutions.

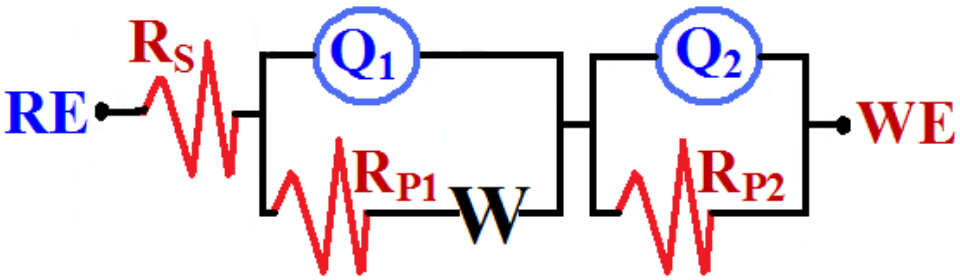

Figure 6. Equivalent circuit model used to fit the EIS Nyquist plots presented in Fig. 5.

It is seen from Table 1 that the values of R_S, R_{P1} and R_{P2} recorded higher values for aluminum coated with PVA and further increment was recorded for aluminum coated with PVC. The CPEs, Q_1 with its n values almost 1.0 represent double layer capacitors with some pores; the CPEs decrease, while their *n*-values increase in case of PVA and PVC; this was expected to cover the charged aluminum surfaces and to reduce the capacitive effects. The CPEs, Q_2 with its n value is exactly 1.0 represent another double layer capacitors. The decrease of Q_1 and Q_2 values indicates that the surface is more passivated compared to the aluminum surface without any coatings. The presence of the Warburg impedance (W) gives another confirmation that the corrosion of aluminum in the chloride solutions via mass transport is limited by the top layers of PVA and PVC nanofiber coatings.

Table 1. Impedance parameters obtained by fitting the Nyquist plots shown in Fig. 5 with the equivalent circuit shown in Fig. 6 for Al electrodes after their immersion in 3.5 wt.% NaCl solutions.

Material	Parameter							
	RS / Ω cm2	Q1		RP1 / Ω cm2	W Ω S−1/2	Q2		RP2 / Ω cm2
		YQ1/ µF cm-2	n			YQ2/ µF cm-2	n	
Uncoated Al	34	58.43	0.89	10510	4.31x10−6	0.84	1.00	35860
PVA coated Al	52	46.65	0.94	12170	2.99x10−6	0.33	1.00	163600
PVC coated Al	66	25.99	1.00	14100	1.72x10−6	0.16	1.00	221300

3.4. Cyclic potentiodynamic polarization (CPP) measurements

The CPP measurements were carried out on aluminum surfaces without (a) and with PVA (b) and PVC (c) nanofiber coatings after 20 min immersion in freely aerated stagnant 3.5 wt.% NaCl solutions and the curves are respectively shown in Fig. 7. The values of cathodic (β_c) and anodic (β_a) Tafel slopes, corrosion potential (E_{Corr}), corrosion current (j_{Corr}), pitting potential (E_{Pit}), protection potential (E_{Prot}), polarization resistance (R_P), and corrosion rate (K_{Corr}) obtained from the polarization curves shown in Fig. 7, are listed in Table 2. The values of j_{Corr} and E_{Corr} were obtained from the extrapolation of anodic and cathodic Tafel lines located next to the linearized current regions. The Rp values for aluminum corrosion were calculated from the Stern–Geary equation using the values of β_c,

β_a, and j_{Corr} as reported in our previous work [42-48]. The values of K_{Corr} were calculated from the polarization data as follows [49-52]:

$$K_{Corr} = \frac{j_{Corr}\, k\, E_W}{d\, A} \qquad (1)$$

Where, k is a constant that defines the units for the corrosion rate (= 3272 mm/ (amp.cm.year)), E_W the equivalent weight in grams/equivalent (E_W = 9), d the density in g cm^{-3} (d = 2.7), and A the area of the exposed surface of the Al electrode in cm^2 (A = 1 cm^2).

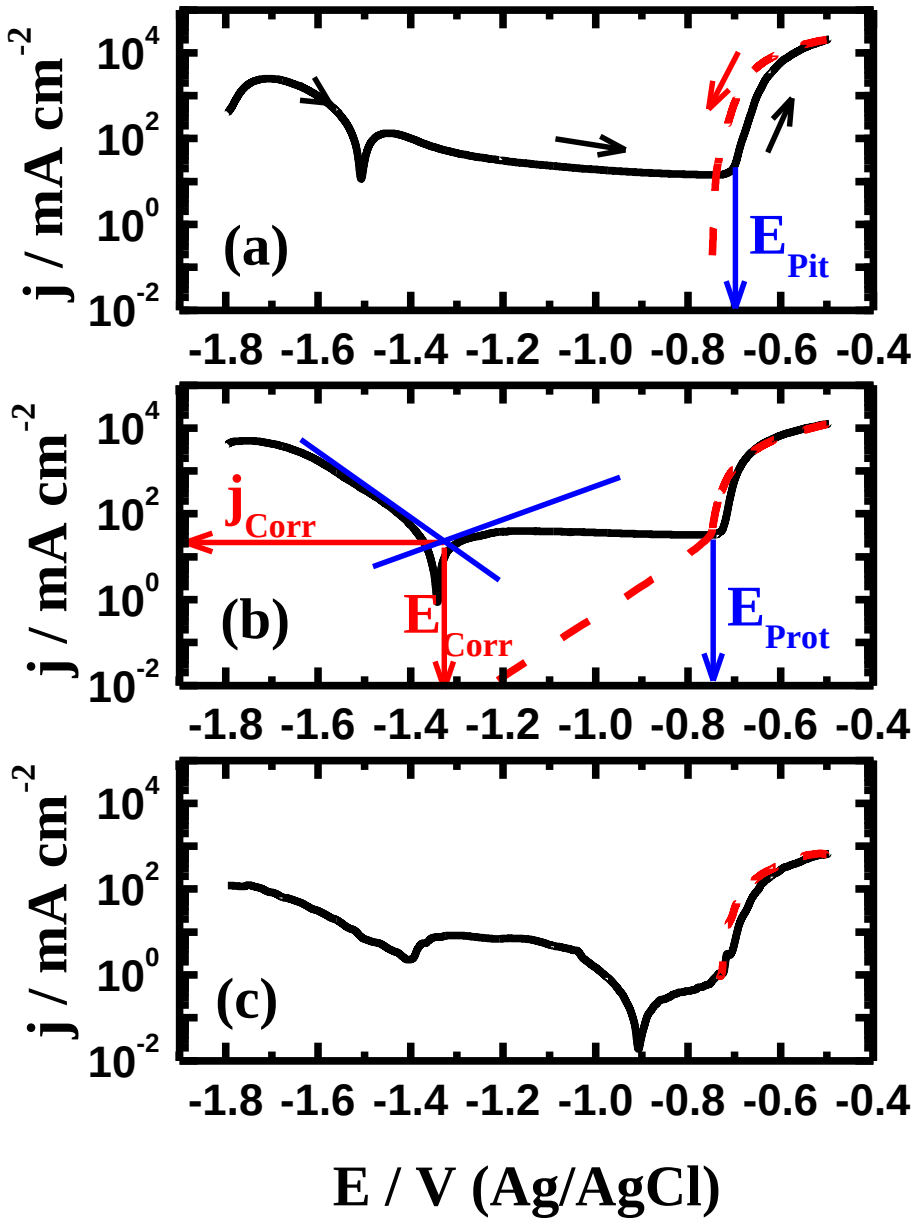

Figure 7. Cyclic potentiodynamic polarization curves obtained for (a) uncoated Al, (b) PVA coated Al, and (c) PVC coated Al electrodes after their immersion for 20 min in freely aerated 3.5 wt.% NaCl solutions.

It has been reported that the cathodic reaction for aluminum in near neutral aerated chloride solutions must be primarily oxygen reduction followed by its adsorption [24,28] *i.e.*

$$\frac{1}{2}O_2 + H_2O_{(S)} + e^- = OH_{ads.} + OH^- \quad (2)$$

and

$$OH_{ads.} + e^- = OH^- \quad (3)$$

On the other hand, the anodic reaction is the combination of aluminum with the hydroxide ions from the solution to form aluminum hydroxide, which transforms at end to hydrated aluminum oxide according to the following equations [24,28],

$$Al_{(S.)ads.} + 3OH^- = Al(OH)_{3,ads.} + 3e^- \quad (4)$$

$$2Al(OH)_{3,ads.} = Al_2O_3 \cdot 3H_2O \quad (5)$$

Table 2. Parameters obtained from polarization curves shown in Fig. 7 for Al electrodes after their immersion in 3.5% NaCl solutions for 20 min before measurement.

Material	Parameter							
	-βc / V dec-1	ECorr / V	jCorr / μA cm-2	βa / V dec-1	EPit / V	EProt / V	Rp / Ω cm2	KCorr / mmy-1
Bare Al	0.11	–1.485	100	0.11	–0.70	-0.745	0.24	1.091
Al coated PVA	0.14	–1.330	22	0.24	–0.72	0.740	1.75	0.2399
Al coated PVC	0.12	–0.890	0.25	0.21	–0.71	-0.730	132.8	0.0027

It is seen from the polarization curve shown in Fig. 7a that the anodic branch exhibits very wide passive region, which is due to the formation of aluminum oxide film, Eq. [4] and Eq. [5]. This oxide film gets thick with increasing the applied potential up to nearly – 760 mV vs. Ag/AgCl. Further increasing the potential to the less negative values led to a rapid increase of the output current for aluminum, where the passive and thick oxide film breakdown occurred. This is due to not only the potential step but also the pitting corrosion of aluminum. At this condition, the dissolution of aluminum proceeds as follows [1,22-28],

$$Al = Al^{3+} + 3e^- \quad (6)$$

The chloride ions attack the weak parts of the oxide film and reach the aluminum surface to form an aluminum chloride soluble complex that goes to the solution causing aluminum pitting corrosion;

$$Al^{3+} + 4Cl^{-} = AlCl_4^{-} \quad (7)$$

In order to confirm that the pitting corrosion occurs for aluminum after the breakdown of the passive film, SEM surface investigation was performed on aluminum surface after the forward anodic potential scan (- 500 mV vs. Ag/AgCl). Fig. 8 shows the SEM micrographs for aluminum surface after 20 min immersion in 3.5 wt.% NaCl solutions, (a) before potential application and (b) after the forward potential scan, respectively. It is clearly seen from Fig. 8a that there is not pitting corrosion observed in the aluminum surface before running the polarization test. On the other hand, the pits are clearly seen in the case of aluminum that was immersed in the chloride solution for 20 min before scanning the potential in the forward direction from -1800 to -500 mV vs. Ag/AgCl as shown in Fig. 8b. This confirms the data obtained by polarization measurements shown in Fig. 7.

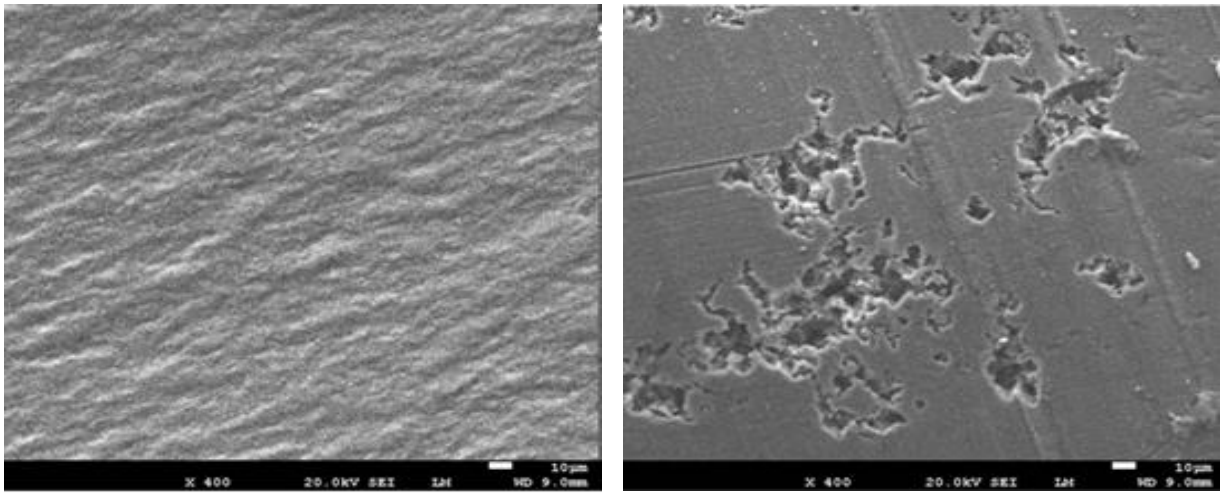

Figure 8. SEM micrographs for aluminum surface after 20 min immersion in 3.5 wt.% NaCl solutions, (a) before potential application and (b) after the forward anodic polarization scan, respectively.

It is also seen from Fig. 7 and Table 1 that the presence of PVA and PVC on top of aluminum electrodes decreased the values of j_{Corr} and K_{Corr} and increased the values of R_P. Furthermore, the PVA and PVC coated aluminum electrodes showed less negative values for E_{Corr}. This indicates that PVA and PVC nanofiber coatings highly precluded the dissolution aluminum via uniform and pitting corrosion in the chloride test solution and the protection efficiency proceeds in the order PVC > PVA.

4. CONCLUSION

The fabrication of two polymer nanofiber coatings, namely polyvinyl alcohol (PVA) and polyvinyl chloride (PVC), was successfully performed in our laboratory. The PVA and PVC coatings were applied on aluminum substrate using the electrospinning technique. The scanning electron

microscope (SEM) was used to examine the surface morphology of the coated and uncoated aluminum. Thermal degradation analysis (TGA) for PVA and PVC was performed to report the thermal stability for PVA and PVC coatings on the aluminum surface. The corrosion passivation of aluminum in 3.5 wt.% NaCl solutions by PVA and PVC was investigated using cyclic potentiodynamic polarization (CPP) and electrochemical impedance spectroscopy (EIS) measurements. The corrosion tests revealed that the aluminum is highly corroded in the chloride solution, while the presence of PVA and PVC coatings on top of aluminum surface greatly precluded this corrosion. Both PVA and PVC shifted the corrosion potential to the very less negative values, decreased the corrosion rate and increased polarization resistance of aluminum in NaCl test solution. Results together are in good agreement with each other showing clearly that the both PVA and PVC nanofiber coatings protect aluminum surface against corrosion in 3.5 wt.% NaCl solution and the protection efficiency is as follows PVC > PVA.

ACKNOWLEDGEMENTS
The authors extend their appreciation to the Deanship of Scientific Research at King Saud University for funding the work through the research group project No RGP-VPP-036.

References

1. M. Es-saheb, A.A. Elzatahry, El-Sayed M. Sherif, A.S. Alkaraki, El-Refaie kenawy, *Int. J. Electrochem. Sci*., 7 (2012) in press.
2. Z.-M. Huang, Y.-Z. Zhang, M. Kotakic, S. Ramakrishna, Compos. Sci. Technol., 63 (2003) 2223.
3. D.H. Renker, Haoqing Hou, Electrospinning. Encyclopedia of Biomaterials Biomedical Engineering, 31 August (2004).
4. D. Luck, A. Sarkar, L. Martinov, K. Vodsed Ikov, D. Lubasov, J Chaloupec, P. Pokorn, P. Mike, J.Chvojka, M. Komrek, *Journal Textile Progress*, 41(2009) 559.
5. Feng-Lei Zhou, Rong-hua Gong, Isaac Porat, *Polymer International*, 58 (2009) 331.
6. J.M. Deitzel, J. Kleinmeyer, J.K. Hirvonen, T.N.C. Beck, *Polymer*, 42 (2001) 8163.
7. S.C. Tjong, Haydn Chen, *Materials Science and Engineering* R, 45 (2004) 1-88.
8. L. Maya, W.R. Allen, *J. Vac. Sci. Technol*., B 13 (2) (1995) 361.
9. F. Vaz, L. Rebouta, *Mater. Sci. Forum*, 383 (2002) 143.
10. S. Veprek, A.S. Argon, *Surf. Coat. Technol.*, 146–147 (2001) 175.
11. R.A. Andrievski, *Mater. Trans. 42*, (2001) 1471.
12. V. Provenzano, R.L. Holtz, *Mater. Sci. Eng. A*, 204 (1995) 125.
13. R.A. Andrievski, A.M. Gleze, *Scripta Mater.*, 44 (2001) 1621.
14. H. Fong, D.H. Reneker In: D.R. Salem, Editor, *Structure formation in polymeric fibers*, Munich, Hanser, (2001) p. 225–46.
15. G.M. Whitesides, B. Grzybowski, *Science*, 295 (2002) 2418.
16. P.X. Ma, R. Zhang, *J. Biomed. Mat. Res.*, 46 (1999) 60.
17. T. Ondarcuhu, C. Joachim, *Europhys. Lett.*, 42 (1998) 215.
18. L. Feng, S. Li, H. Li, J. Zhai, Y. Song, L. Jiang, et al., *Angew Chem. Int. Ed.*, 41 (2002) 1221.
19. Th. Lampke, A. Leopold, D. Dietrich, G. Alisch, B. Wielage, *Surf. Coat. Technol.*, 201 (2006) 3510.
20. R. C. Agaewala, V. Agarwala, Electroless alloy/composite coatings: A review, *Sadhana*, 28 part 3 & 4 (2003) 475.

21. Sam Zhang, Deen Sun, Yongqing Fu, Hejun Du, *Surf. Coat. Technol.*, 167 (2003) 113.
22. El-Sayed M. Sherif, F.H. Latif, H. Junaedi, A.A. Almajid, *Int. J. Electrochem. Sci.,* 7 (2012) 4352.
23. El-Sayed M. Sherif, A.A. Almajid, F.H. Latif, H. Junaedi, *Int. J. Electrochem. Sci.,* 6 (2011) 1085
24. E.M. Sherif, S.-M. Park, *Electrochim. Acta,* 51 (2006) 1313.
25. El-Sayed M. Sherif, E.A. El-Danaf, M.S. Soliman, A.A. Almajid, *Int. J. Electrochem. Sci.,* 7 (2012) 2846.
26. El-Sayed M. Sherif, *Int. J. Electrochem. Sci.* 6 (2011) 1479.
27. F.H. Latief, El-Sayed M. Sherif, A.A. Almajid, H. Junaedi, *J. Anal. Appl. Pyrolysis,* 92 (2011) 485.
28. E.M. Sherif, S.-M. Park, *J. Electrochem. Soc*., 152 (2005) B205.
29. El-Sayed M. Sherif, *J. Appl. Surf. Sci*., 252 (2006) 8615.
30. El-Sayed M. Sherif, Corrosion Inhibition in Chloride Solutions of Iron by 3-Amino-1,2,4-triazole-5-thiol and 1,1'-Thiocarbonyldiimidazole, *Int. J. Electrochem. Sci.*, 7 (2012) In Press.
31. El-Sayed M. Sherif, *Int. J. Electrochem. Sci.*, 6 (2011) 3077.
32. El-Sayed M. Sherif, *Int. J. Electrochem. Sci.*, 7 (2012) 1482.
33. El-Sayed M. Sherif, Effects of 3-Amino-1,2,4-triazole-5-thiol on the Inhibition of Pure Aluminum Corrosion in Aerated Stagnant 3.5 wt.% NaCl Solution as a Corrosion Inhibitor, *Int. J. Electrochem. Sci.*, 7 (2012) In Press.
34. El-Sayed M. Sherif, *J. Mater. Eng. Performance,* 19 (2010) 873.
35. El-Sayed M. Sherif, A.H. Ahmed, *Synthesis and Reactivity in Inorganic, Metal-Organic, and Nano-Metal Chemistry*, 40 (2010) 365.
36. El-Sayed M. Sherif, R.M. Erasmus, J.D. Comins, *J. Appl. Electrochem.,* 39 (2009) 83.
37. H. Ma, S. Chen, L. Niu, S. Zhao, S. Li, D. Li, *J. Appl. Electrochem*., 32 (2002) 65.
38. El-Sayed M. Sherif, *Int. J. Electrochem. Sci.*, 7 (2012) 2374.
39. El-Sayed M. Sherif, J. H. Potgieter, J. D. Comins, L. Cornish, P. A. Olubambi, C. N. Machio, J. Appl. Electrochem. 39 (2009) 1385.
40. El-Sayed M. Sherif, *J. Solid State Electrochem.,* 16 (2012) 891.
41. El-Sayed M. Sherif, *Int. J. Electrochem. Sci.*, 7 (2012) 1884.
42. E.M. Sherif, S.-M. Park, Electrochim. Acta 51 (2006) 4665.
43. Khalil A. Khalil, El-Sayed M. Sherif, A.A. Almajid, *Int. J. Electrochem. Sci.,* 6 (2011) 6184.
44. El-Sayed M. Sherif, *Int. J. Electrochem. Sci*., 6 (2011) 2284.
45. El-Sayed M. Sherif, A.A. Almajid, A.K. Bairamov, Eissa Al-Zahrani, *Int. J. Electrochem. Sci.*, 6 (2011) 5430.
46. El-Sayed M. Sherif, A.A. Almajid, A.K. Bairamov, Eissa Al-Zahrani, *Int. J. Electrochem. Sci.,* 7 (2012) 2796.
47. E.M. Sherif, S.-M. Park, *Electrochim. Acta,* 51 (2006) 6556.
48. E.M. Sherif, S.-M. Park, *J. Electrochem. Soc*., 152 (2005) B428.
49. El-Sayed M. Sherif, *Int. J. Electrochem. Sci.*, 7 (2012) 2832.
50. E. M. Sherif, S.-M. Park, *Corros. Sci.,* 48 (2006) 4065.
51. El-Sayed M. Sherif, A.A. Almajid, *J. Appl. Electrochem.,* 40 (2010) 1555.
52. El-Sayed M. Sherif, R.M. Erasmus, J.D. Comins, *Electrochim. Acta,* 55 (2010) 3657.